

Scaling of thermal conductivity of helium confined in pores

Kwangsik Nho and Efstratios Manousakis

Department of Physics and MARTECH, Florida State University, Tallahassee, Florida 32306

(Received 8 March 2001; published 21 September 2001)

We have studied the thermal conductivity of confined superfluids on a barlike geometry. We use the planar magnet lattice model on a lattice $H \times H \times L$ with $L \gg H$. We have applied open boundary conditions on the bar sides (the confined directions of length H) and periodic along the long direction. We have adopted a hybrid Monte Carlo algorithm to efficiently deal with the critical slowing down and in order to solve the dynamical equations of motion we use a discretization technique which introduces errors only $O[(\delta t)^6]$ in the time step δt . Our results demonstrate the consistency of scaling using known values of the critical exponents and we obtained the scaling function of the thermal resistivity. We find that our results for the thermal resistivity scaling function are in very good agreement with the available experimental results for pores using the temperature scale and thermal resistivity scale as free fitting parameters.

DOI: 10.1103/PhysRevB.64.144513

PACS number(s): 64.60.Fr, 67.40.Kh

I. INTRODUCTION

The superfluid transition of liquid ^4He offers a unique opportunity for testing the finite-size scaling theory of static and dynamic critical phenomena. Recently, a sophisticated experimental study was carried out in microgravity environment, the so-called confined helium experiment (CHeX). Lipa *et al.*¹ measured the specific heat of helium confined in a parallel plate geometry with a spectacular nanokelvin resolution, thus, providing experimental results within a few nanokelvin of T_λ . When the critical temperature is approached, the bulk correlation length ξ of the fluid can become of the order of the confining length. CHeX approached so close to the lambda point that the correlation length became macroscopic in size. In this case the whole fluid acts in a correlated way and this changes the value of global properties, such as the specific heat, relative to their bulk values. In a parallel approach, Mehta and Gasparini^{2,3} have also reported earth-bound measurements on samples with smaller plate spacing L . The size of L used in these measurements is smaller so that the results are not significantly influenced by the change in T_λ between the top and bottom of the film because of hydrostatic pressure difference which exists due to the earth's gravitational field.

The finite-size scaling (FSS) theory⁴ and the renormalization-group theory⁵ (RGT) were expected to describe the behavior of the system at temperature close to T_λ . A testable implication of this theory is that very close to the lambda point, in a confined system with a confining length of size H , a dimensionless quantity or the ratio of two quantities having the same dimensions, is only a function of the ratio of ξ/H . Therefore the values of a given observable $O(t, H)$, for various values of H and of the reduced temperature $t = |1 - T/T_\lambda|$, divided by its bulk value of $O(t, H = \infty)$ should be a dimensionless scaling function $f(x)$, where $x = \xi(t)/H$. The results of CHeX were in remarkable agreement with predictions which were available prior to the experiment based on scaling functions obtained from renormalization-group theory⁶⁻⁸ and those obtained by combining FSS and the results obtained from large-scale simulations.⁹

A second equally important step toward understanding the

FSS theory is to study dynamical and transport properties near a critical point. A well-suited candidate problem for this study is the thermal conductivity λ of ^4He near T_λ . When T_λ is approached from above, the thermal conductivity of the fluid diverges.^{10,11} The precise behavior of bulk λ as a function of t was studied in great detail both experimentally¹²⁻¹⁴ and theoretically.¹⁵

There are several recent theoretical studies of dynamical critical phenomena and dynamical scaling. Koch, Dohm, and Stauffer¹⁶ presented field-theoretical and numerical studies of the validity of dynamic finite-size scaling for relaxational dynamics in cubic geometry with periodic boundary conditions above and below T_c . Quantitative agreement between theory and Monte Carlo data was obtained by them. Koch and Dohm¹⁷ have provided a prediction for the dynamic finite-size scaling function for the effective diffusion constant of model C of Hohenberg and Halperin.¹⁸ Bhattacharjee¹⁹ derived an approximate form of the scaling function for the thermal conductivity using a decoupled-mode approximation and model E . Krech and Landau²⁰ calculated the transport coefficient of the out-of-plane magnetization component at the critical point, which is related to the thermal conductivity of liquid ^4He using Monte Carlo spin dynamics simulations of the XY model in three dimensions on a simple cubic lattice with periodic boundary conditions. They determined the critical exponent characterizing the thermal conductivity.

Accurate experimental studies have been carried out not only for dynamic bulk phenomena with improved resolution but also dynamic properties *in confined geometries* deeply in the critical region.^{21,22} Rather recently, Kahn and Ahlers²³ measured the thermal conductivity of liquid ^4He confined in a glass capillary array of thickness 3 mm with holes 2 μm in diameter. Their results show that long cylindrical samples have a transition from three-dimensional to one-dimensional behavior and there is no phase transition in the one-dimensional system. However, as measurements over a wide range of hole-diameter are required in order to test the finite-size scaling theory for transport properties, further experimental studies are planned²⁴ in order to reveal dynamical exponents near the critical point and to study the finite-size

scaling behavior of the thermal conductivity in such confining geometries. To avoid the limitations imposed by the earth's gravity, this experimental effort²⁴ will be carried out under microgravity conditions on the Low Temperature Microgravity Facility on International Space Station.

In this paper we wish to study the thermal conductivity λ of confined helium and to calculate the scaling function associated with λ for a fixed geometry. Since there are already experimental results²³ for the scaling function of λ for the pore-like geometry, in this paper we will focus our attention to this geometry because we hope to compare with the experiment. We will examine the FSS theory for the thermal conductivity of helium confined in a barlike geometry, i.e., on an $H^2 \times L$ lattice with $L \gg H$. This confining geometry is similar to that of Kahn and Ahlers²³ because two of the dimensions of a pore used in their experimental studies are confining as is the case of the barlike geometry. We will consider the limit in which our results are independent of the bar length L . We will apply periodic boundary conditions (BC) in the L direction because these BC approach the bulk limit faster. In the other two directions which are kept finite we will apply open boundary conditions. We will use the dynamics of planar-magnet model and Monte Carlo simulation to study $\lambda(t, H)$. We find that $\lambda(t, H)H^{-\pi/\nu}$ plotted as a function of $x = tH^{1/\nu}$ fall on the same curve for a wide range of values of H and t , using the known values of ν and π . This demonstrates that finite-size scaling is also valid for dynamical critical properties. In addition we obtain the scaling function which fits very well the experimental data of Kahn and Ahlers²³ using the scale of temperature and the thermal conductivity scale as free parameters.

II. THE METHOD

We will first briefly describe the model and the numerical method used and show how the thermal conductivity is computed in our model. To describe the dynamics of a superfluid, we will use the planar magnet model which is classified as model F (or E in the absence of an external field) by Hohenberg and Halperin.¹⁸ Matsubara and Matsuda²⁵ has proposed model F to explain the properties of liquid ^4He . The problem of hard core bosons can be described by a lattice gas model which can be mapped to the quantum antiferromagnet in which the superfluid order parameter corresponds to $S_x - iS_y$ while the density of the boson system corresponds to $1/2 - S_z$. In order to study equilibrium critical properties of a superfluid one uses the XY model^{9,26} because the planar magnet model and the XY model belong to the same universality class.²⁷ For critical dynamics of a superfluid, however, one needs to use the full planar magnet model in which the role of the third component of the pseudospin is crucial.¹⁸

In the pseudospin notation, the planar magnet model takes the following form:

$$H = -J \sum_{\langle ij \rangle} (S_i^x S_j^x + S_i^y S_j^y), \quad (1)$$

where the summation is over all nearest neighbors, $\vec{S}_i = (S_i^x, S_i^y, S_i^z)$, and J sets the energy scale. In the usual XY

model the two-component pseudomagnetization corresponds to the superfluid order parameter. In the planar magnet model, the third component corresponds to the particle density and it is necessary in order to study the dynamics.

In our calculations, we use a barlike geometry, i.e., a $H \times H \times L$ lattice with $L \gg H$. This geometry is chosen in order to mimic the pore geometry used in experimental studies. In our calculations, open boundary conditions are imposed in the H direction, and in the L direction we applied periodic boundary conditions. In open or free boundary conditions the order parameter is allowed to take any value at the boundaries. In our pseudospin model this means that the spins at the boundary have no neighbors outside the confining space.

We use a hybrid Monte Carlo procedure²⁰ which consists of a combination of steps using the Metropolis update, the Cluster update,²⁸ and the over-relaxation algorithm.²⁹ Using this hybrid algorithm, we generate approximately 3000-10 000 uncorrelated configurations from the equilibrium canonical ensemble at a given temperature. Each configuration is evolved using the equations of motion for the planar magnet model which are given as follows:^{20,18}

$$\frac{d}{dt} \vec{S}_i = \frac{\partial H}{\partial \vec{S}_i} \times \vec{S}_i. \quad (2)$$

Starting from a particular initial spin configuration, we perform numerical integration of these equations of motion. Following Ref. 30 we use a recently developed decomposition method³¹ where the integration is carried out to a maximum time t_{\max} (typically of the order of $t_{\max} = 400$) with a time step $\delta t = 0.05$. We made sure that this way we determined the real-time history of every configuration within a sufficiently long interval of time ($0 \leq t \leq t_{\max}$). Finally, we compute the thermal average of a time-dependent observable (such as the thermal current-current correlation function) by averaging over all the values of the observable obtained by evolving all the independent initial equilibrium configurations generated via the hybrid Monte Carlo procedure.

Compared to calculating static critical properties, the computation of dynamical properties is far more CPU time intensive and demands large computational resources. The computations described here were carried out on a dedicated massively parallel cluster of 64 CPUs which was designed by our group to achieve high performance to cost ratio.

We computed the thermal conductivity on $H \times H \times L$ lattices, where $H = 6, 8, 10, 12, 14, 20$ and $L = 5H$. The thermal conductivity λ of liquid ^4He at a given temperature T can be calculated using the dynamic current-current correlation function²⁰

$$\lambda = \frac{1}{k_B T \chi_{zz}} \frac{2}{\pi} \int_0^\infty dt \sum_i \langle j_0^z(0) j_i^z(t) \rangle, \quad (3)$$

where the out-of-plane static susceptibility

$$\chi_{zz} = \langle M^z \rangle / (k_B T L^3) \quad (4)$$

is needed for normalization. The z component j_i^z of the current density \vec{j}_i associated with the lattice point i is defined by

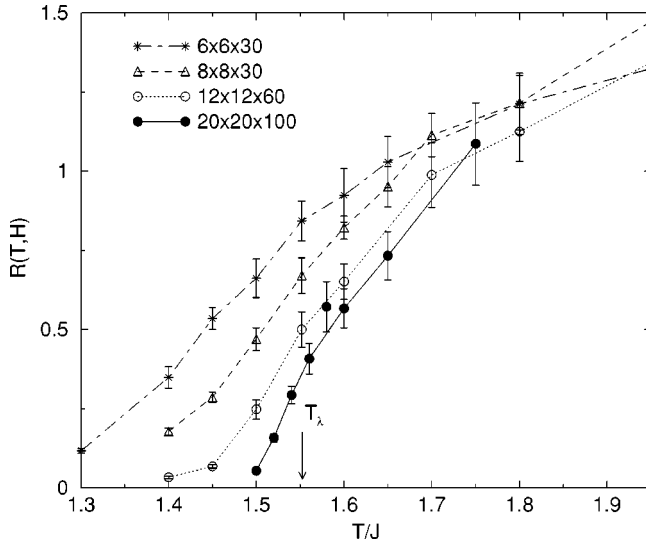


FIG. 1. Thermal resistivity $R(T,H)$ versus temperatures for bar-like lattices with sizes that correspond to $H=6,8,12,20$ and $L=5H$. The bulk $T_\lambda=1.5518$ is also shown.

$$j_i^z = J(S_i^y S_{i+e_z}^x - S_i^x S_{i+e_z}^y), \quad (5)$$

where the notation $i+e_z$ denotes the nearest neighbor of the lattice site i in the z lattice direction.

Now, we would like to examine the finite-size scaling hypothesis for the thermal resistivity $R(t,H)=1/\lambda(t,H)$, and to compare our results with the existing experimental results.²³ The dependence upon t of the bulk thermal resistivity can be described by the power law

$$R(t) = R_0 t^\pi, \quad (6)$$

where π is a dynamic critical exponent. Using Eq. (6), the finite-size scaling expression for the thermal resistivity $R(t,H)$ is given by

$$R(t,H)H^{\pi/\nu} = f(tH^{1/\nu}), \quad (7)$$

where the function $f(x)$ is universal and $\nu=0.6705$ is the critical exponent of the correlation length.³²

III. RESULTS

In this section, we calculate the thermal resistivity, we examine its scaling behavior with respect to H and then we compare the scaling function with the experimental results. To calculate these observables with small statistical errors even with our utilization of the most recent numerical advances and with using the 64-node dedicated cluster, it requires significant amount of time of high-throughput computation.

Figure 1 shows some of our results for the thermal resistivity $R(T,H)$ as a function of temperature T for various lattice sizes with open boundary conditions in the H direction. Our results for $R(T,H)$ for several values of H and T are given in Tables I and II. We wish to make L large enough so that finite-size effects due to L are smaller than our statistical errors. We have found that taking $L \approx 5H$ and applying

TABLE I. Calculated results for the thermal resistivity for lattices $H \times H \times L$ with $L \approx 5H$ and $H=6,8,10,12,14$. The number in parenthesis gives the error in the last decimal places.

T/J	$H=6$	$H=8$	$H=10$	$H=12$	$H=14$
1.40	0.350(34)	0.178(11)	0.053(4)	0.033(4)	
1.45	0.535(35)	0.286(17)	0.143(10)	0.068(6)	0.050(4)
1.50	0.662(61)	0.470(36)	0.353(38)	0.247(31)	0.182(21)
1.5518	0.843(62)	0.670(56)	0.614(53)	0.501(56)	0.452(59)
1.60	0.923(84)	0.821(36)	0.688(67)	0.652(55)	0.706(42)
1.65	1.028(81)	0.951(64)	0.854(42)		
1.70		1.114(69)	0.901(63)	0.988(102)	0.984(105)
1.80	1.213(97)	1.216(86)		1.125(94)	1.081(166)

periodic boundary conditions along the direction of L introduces insignificant finite size effects due to the finite size of L for the temperature range studied here. Our calculations are applicable in the region for which the correlation length is large but smaller than L . We wish to explore the region where $\xi(t)$ can become comparable and even larger than H but still smaller than L . Namely our calculation should be restricted in the region where our results for R do not to feel the size effects due to the finiteness of L . Since $L=5H$ there is a significant region of our dimensionless parameter $\xi(t)/H$ where the condition $\xi(t) < L$ is satisfied. Most of the experimentally probed region is covered by this region where our calculation is “safe.”

Notice in Fig. 1 that the thermal resistivity feels strong finite-size effects due to the bar thickness H . The arrow shows the bulk transition temperature $T_\lambda=1.5518$ obtained from Monte Carlo simulation using the planar magnet model.²⁷ In bulk helium $R(t)$ approaches zero as the bulk transition temperature T_λ is approached from above.

We wish to avoid using any adjustable parameters to obtain scaling of our results. Thus, we need to examine if our results obey scaling using the known values of the critical exponents ν and π . The value of ν is accurately known from theoretical and experimental studies of static critical properties and we shall use the value $\nu=0.6705$ as determined by Goldner and Ahlers.³² There is less agreement between theory and experiment on the actual value of the dynamical critical exponent π . Ahlers³³ used a power law fit to the data of Tam and Ahlers¹² for their “Cell F ” and he found the

TABLE II. Calculated results for the thermal resistivity for an $20 \times 20 \times 100$ size lattice.

T/J	$H=20$
1.50	0.053(3)
1.52	0.158(13)
1.54	0.294(27)
1.56	0.408(48)
1.58	0.572(79)
1.60	0.567(62)
1.65	0.733(76)
1.75	1.086(130)

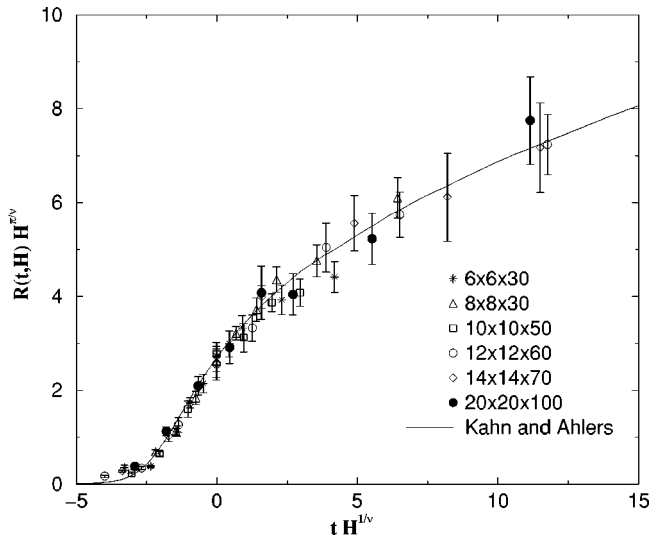


FIG. 2. The universal function $f(x)$ obtained for barlike geometry. The solid line represents the available experimental results for porelike geometry. In the experimental results the resistivity scale and the temperature scale are used as free parameters.

value $\pi=0.4397$. On the other hand the dynamic scaling theory³⁴ had predicted a divergence in λ with a critical exponent given by $\pi=\nu/2\approx 0.335$. However, renormalization-group calculations¹⁵ can explain quantitatively the difference between the experimental effective exponent $\pi=0.44$ and the asymptotic exponent $\pi=\nu/2$ in terms of non-universal corrections to the asymptotic critical behavior which vanish extremely slowly as t vanishes.

Figure 2 shows a scaling plot of the thermal resistivity scaling function $f(x)=R(t,H)t^{\pi/\nu}$ versus the scaled reduced temperature parameter $x=tH^{1/\nu}$, where the reduced temperature is taken relative to the bulk transition temperature T_λ . Our Monte Carlo data collapse onto a universal curve using

the value of $\pi\approx 0.44$ determined by Ahlers.³³ In Fig. 2 we compare our universal function $f(x)$ with the experimental data obtained by Kahn and Ahlers²³ represented by a solid line. In order to do this, we used two multiplicative constants as free fitting parameters, one multiplying the scale of x axis and another the scale of y . The agreement between Monte Carlo simulation and experiment is quite satisfactory. In the past it has been demonstrated^{26,35} that the boundary conditions play a significant role in defining the universal function $f(x)$. We believe that if we use more realistic boundary conditions, such as Dirichlet boundary conditions, along the H direction we can reduce the number of fitting parameters to only one.

Our results are expected to scale using the same effective critical exponent and not with the asymptotic exponent. Using the asymptotic value of $\pi=\nu/2$, the results of our simulation also collapse (within our error bars) on a different scaling function. However, if we attempt to fit the scaling curve with the experimental resistivity of Kahn and Ahlers we obtain a lower quality fit than that of Fig. 2.

In summary we have calculated the thermal resistivity $R(t,H)$ of liquid ^4He in a porelike geometry (on a $H\times H\times L$ lattice) applying open boundary conditions in the H direction. We have been able to demonstrate the validity of finite-size scaling theory and we obtained the thermal resistivity scaling function $f(x)$ using known values for the critical exponents and no adjustable parameters. In addition, the scaling function $f(x)$ for $R(t,H)$ agrees rather well with experimental data using the temperature scale and thermal resistivity scale as free parameters.

ACKNOWLEDGMENTS

This work was supported by the National Aeronautics and Space Administration under Grant No. NAG3-1841 and NAG8-1773.

¹J. A. Lipa *et al.*, Phys. Rev. Lett. **84**, 4894 (2000); J. A. Lipa, D. R. Swanson, J. A. Nissen, Z. K. Greg, P. R. Williamson, D. A. Stricker, T. C. P. Chui, U. E. Israelsson, and M. Larsen, J. Low Temp. Phys. **113**, 849 (1998).

²S. Mehta and F. M. Gasparini, Phys. Rev. Lett. **78**, 2596 (1997).

³S. Mehta, M. O. Kimball, and F. M. Gasparini, J. Low Temp. Phys. **114**, 467 (1999).

⁴M. E. Fisher and M. N. Barber, Phys. Rev. Lett. **28**, 1516 (1972); M. E. Fisher, Rev. Mod. Phys. **46**, 597 (1974); V. Privman, *Finite Size Scaling and Numerical Simulation of Statistical Systems* (World Scientific, Singapore, 1990).

⁵M. E. Fisher, Rev. Mod. Phys. **70**, 653 (1998); V. Dohm, Phys. Scr. **T49**, 46 (1993).

⁶E. Brezin, J. Phys. (France) **43**, 15 (1982).

⁷F. M. Gasparini and I. Rhee, in *Progress in Low Temperature Physics XIII*, edited by D. F. Brewer (North-Holland, Amsterdam, 1992), p. 1.

⁸R. Schmolke, A. Wacker, V. Dohm, and D. Frank, Physica B **165&166**, 575 (1990); V. Dohm, Phys. Scr. **T49**, 46 (1993).

⁹N. Schultka and E. Manousakis, Phys. Rev. Lett. **75**, 2710 (1995).

¹⁰G. Ahlers, Phys. Rev. Lett. **21**, 1159 (1968).

¹¹J. Kerrisk and W. E. Keller, Phys. Rev. **177**, 341 (1969).

¹²W. Y. Tam and G. Ahlers, Phys. Rev. B **32**, 5932 (1985).

¹³M. Dingus, F. Zhong, and H. Meyer, J. Low Temp. Phys. **65**, 185 (1986).

¹⁴W. Y. Tam and G. Ahlers, Phys. Rev. B **33**, 183 (1986).

¹⁵B. I. Hohenberg and E. D. Siggia, Phys. Rev. Lett. **32**, 1289 (1974); Phys. Rev. B **13**, 1299 (1976); E. D. Siggia, *ibid.* **13**, 3218 (1976); C. DeDominicis and L. Peliti, Phys. Rev. Lett. **38**, 505 (1977); Phys. Rev. B **18**, 353 (1978); V. Dohm, Z. Phys. B: Condens. Matter **31**, 327 (1978); R. A. Ferrell and J. K. Bhattacharjee, Phys. Rev. Lett. **42**, 1638 (1979); J. Low Temp. Phys. **36**, 165 (1979); P. C. Hohenberg, B. I. Halperin, and D. R. Nelson, Phys. Rev. B **22**, 2373 (1980); V. Dohm and R. Folk, Z. Phys. B: Condens. Matter **40**, 79 (1980); Phys. Rev. Lett. **46**, 349 (1981); G. Ahlers, P. C. Hohenberg, and A. Kornblit, *ibid.* **46**, 493 (1981); Phys. Rev. B **25**, 3136 (1982); V. Dohm and R. Folk, Z. Phys. B: Condens. Matter **45**, 129 (1981); V. Dohm,

- Phys. Rev. B **44**, 2697 (1991).
- ¹⁶W. Koch, V. Dohm, and D. Stauffer, Phys. Rev. Lett. **77**, 1789 (1996).
- ¹⁷W. Koch and V. Dohm, Phys. Rev. E **58**, R1179 (1998).
- ¹⁸P. C. Hohenberg and B. I. Halperin, Rev. Mod. Phys. **49**, 435 (1977).
- ¹⁹J. K. Bhattacharjee, Phys. Rev. Lett. **77**, 1524 (1996).
- ²⁰M. Krech and D. P. Landau, Phys. Rev. B **60**, 3375 (1999).
- ²¹J. A. Lipa and T. C. P. Chui, Phys. Rev. Lett. **58**, 1340 (1987); T. C. P. Chui, Q. Li, and J. A. Lipa, Jpn. J. Appl. Phys. **26**, Suppl. 26-3, 371 (1987).
- ²²G. Ahlers and R. V. Duncan, Phys. Rev. Lett. **61**, 846 (1988).
- ²³A. M. Kahn and G. Ahlers, Phys. Rev. Lett. **74**, 944 (1995).
- ²⁴G. Ahlers and F. C. Liu (private communication).
- ²⁵T. Matsubara and H. Matsuda, Prog. Theor. Phys. **16**, 416 (1956); **16**, 569 (1956); **17**, 19 (1957).
- ²⁶N. Schultka and E. Manousakis, Phys. Rev. B **49**, 12 071 (1994); **51**, 11 712 (1995); J. Low Temp. Phys. **109**, 733 (1997).
- ²⁷K. Nho and E. Manousakis, Phys. Rev. B **59**, 11 575 (1999).
- ²⁸U. Wolff, Phys. Rev. Lett. **62**, 361 (1989).
- ²⁹F. R. Brown and T. J. Woch, Phys. Rev. Lett. **58**, 2394 (1987).
- ³⁰M. Krech, A. Bunker, and D. P. Landau, Comput. Phys. Commun. **111**, 1 (1998).
- ³¹J. Frank, W. Huang, and B. Leimkuhler, J. Comput. Phys. **133**, 160 (1997).
- ³²L. S. Goldner and G. Ahlers, Phys. Rev. B **45**, 13 129 (1992).
- ³³G. Ahlers, J. Low Temp. Phys. **115**, 143 (1999).
- ³⁴R. A. Ferrell, N. Menyhard, H. Schmidt, F. Schwabl, and P. Szepfalusy, Phys. Rev. Lett. **18**, 891 (1967).
- ³⁵N. Schultka and E. Manousakis, Phys. Rev. B **52**, 7528 (1995).